Journal of Applied Mathematics and Computation, 2022, 6(3), 310-331
https://www.hillpublisher.com/journals/JAMC/
ISSN Online: 2576-0653
ISSN Print: 2576-0645

Impact of Optimal Control Techniques on Dual-Bilinear Treatment Protocols for COVID-19 Pandemic

Bassey Echeng Bassey

Department of Mathematics, Cross River University of Technology, Calabar, Nigeria.

How to cite this paper: Bassey Echeng Bassey. (2022) Impact of Optimal Control Techniques on Dual-Bilinear Treatment Protocols for COVID-19 Pandemic. *Journal of Applied Mathematics and Computation*, 6(3), 310-331.
DOI: 10.26855/jamc.2022.09.004

Received: June 22, 2022
Accepted: July 18, 2022
Published: August 9, 2022

***Corresponding author:** Bassey Echeng Bassey, Department of Mathematics, Cross River University of Technology, Calabar, Nigeria.
Email: echengba.rexson@yahoo.com

Abstract

In enacting the goal for possible eradication of the budding COVID-19 pandemic and acknowledging the presence of epileptic availability and uncertain potent of vaccines, the present study adopted and extended the model by Bassey and Atsu (2021) to investigate the impact of optimal control protocols for the treatment dynamics of COVID-19 infection. Initiated by the transformation of the basic model to an optimal control problem, optimal characterization of the model was investigated followed by the establishment of the existence of optimal controls for COVID-19 pandemic. The study explored classical Pontryagin's maximum principle with the incorporation of Hessian matrix for the investigation and analysis of model optimality system and its uniqueness of solutions. Using in-built Runge-Kutta of order of precision 4 in a Mathcad surface, we further presented numerical validations of established theoretical predictions. Results of numerical simulations indicated that with the application of optimal control technique under dual-bilinear optimal control functions, maximal reduction of COVID-19 transmission was highly achieved within 3-18 days with insignificant resurgence of the viral load thereafter. The study therefore, affirmed that under sustained cogent adherence to designated dual-bilinear optimal controls, optimal control technique is an efficient tool for the methodological control of COVID-19 and its related infectious diseases.

Keywords

Hamiltonian-Argument, Pontryagin's-Maximum-Principle, Two-Point-Boundary-Value- Problem, Optimal-Control -Protocols, Dual-Bilinear-Control-Functions

1. Introduction

As at late December, 2019, the global burden of the world was further aggravated following the sudden outbreak of yet another dehumanizing deadly disease known as Coronavirus 2019, codename "COVID-19". The virus, which established its presence first in the city of Wuhan, China, was as at 27th February, 2020, declared a pandemic following the exponential spread of the disease [1]. COVID-19 have become an integral part of nearly every households following its vast spread to over 213 countries and territories with epicenters' at USA, Italy, Spain, Francis, Brazil, Iran, Russia, Egypt, South-Africa and Nigeria [2, 3]. In reality, the extend of devastation cannot be exactly ascertain as casualties are still ongoing but with total matching estimated cases of 42 million infected population and over 1.1 million death toll [4, 5]. The viral load of COVID-19 exhibits varying incubation period ranging between 2-14 days, which makes it possible to accommodate large number of asymptotic patients who could be infectious but with less clinical manifestations and having the most vulnerable

as the elderly of age $\geq 65 years$ [6-8].

Understanding the transmission and control intervention dynamics have been made feasible among other methods through the use of mathematical modeling, which have become an important tool in the analysis and treatment controls of infectious diseases in the form of HVB, HIV, cancer, tuberculosis, zika, Ebola virus, etc. [9]. In the case of Coronavirus for instance, amidst its outbreak, several notable mathematical models have been formulated, which are geared towards understanding the viral load transmission and control dynamics. Such models include [10], which uses the SEIR model for the estimation of the spread of COVID-19 in China. The study [11] formulated an intense generalized SIER model with the incorporation of intrinsic impact of hidden exposed and infectious COVID-19 cases. The use of ordinary differential equations and Markov Chain Monte Carlo methods (MCMC) to estimate the transmission risk and implication of public health intervention was conducted by [12]. The result, which gave an insight to COVID-19 infection dynamics was a leeway towards the annihilation of the deadly disease. Among these waves of mathematical models for COVID-19 dynamics, is our recent model – an 8-Dimensional deterministic compartmental mathematical COVID-19 dynamic model [8]. This model accounted for the global stability analysis of the role of multi-therapies and non-pharmaceutical treatment protocols for COVID-19 pandemic. The study unveiled an insight to the drastic reduction in the spread of COVID-19 following coherent and cogent application of designated dual-bilinear control functions. More importantly, is the recommendation that follows that investigation, which had emphasized on the application of articulated optimal control strategy for possible maximization of the susceptible population.

Notably, optimal control theory has often been applied to infectious disease control in most situation where outright eradication has not been achieved. The study [13] stress the importance of optimal control strategy as a tool for the prediction, forecasting, estimating and making best decision in a disease dynamical system in relation to disease knowledgeable epidemiological characterization. Some notable optimal control model on COVID-19 includes [9] which formulated an optimal policies for the novel coronavirus disease outbreak. The model adopted a multi-objective genetic algorithm for the design of two optimal policies. The result proffered some resourceful policies and as well, addresses economic consequences of applying the proposed optimal policies in the control of COVID-19 infection. The model [3] had proposed and studied optimal control strategy in curtailing the transmission of COVID-19. Considered in that study, were all possible cases of human-to-human transmission under different control strategies and studied using optimal control strategies. The results that follow indicated that quarantine and better medical treatment of the infected individual can reduce the number of critically-infected cases, risk of transmission and mortality rate. In Indonesia, [14] deployed optimal control for the investigation of mathematical model for progression pattern of coronavirus disease. The study adopted the SEI2RS method using five control measures. Results showed that the scenario under large-scale social restriction, contact tracing, case detection and treatment and wearing of face-masks is the most rational scenario in the control of COVID-19 in Indonesia. Still on COVID-19 models, other notable models can be found in [15-18].

Arguably, extol by the importance of optimal control strategy and prompted by the strong suggestion from our earlier study, we present as an extended version of model [8], an optimal control treatment approach for COVID-19 infection under designated dual-bilinear control functions. Explicitly, the novelty of this present study is in the transformation of the model by [8] to an optimal control problem with the objective of maximizing predominant state variables, while minimizing the infectious viral load at a possible minimal systemic cost following the application of dual-bilinear control functions (dual non-pharmaceutical: face-masking and social distancing and dual pharmaceutical: hydroxylchloroquine and azithromycin). Also, the study is the first in the application of optimal control techniques under dual-bilinear control conditions.

Thus, the present study has been partition into 7 sections with Section 1 devoted to the introductory aspect. Section 2 focuses on the study material and methods, which is constituted by the system problem statement and the formulation of an optimal control problem. The mathematical optimal characterization of the optimal system is analyzed in Section 3. In Section 4, we derive and investigate the model optimality system and its uniqueness. Our theoretical predictions are numerically validated in Section 5. The discussion and analysis of obtained results are presented in Section 6. Finally, optimal conclusion and succinct remarks are domicile in Section 7. Thoughtfully, the present study is anticipated to project predictions and resourceful decisions in the quest for complete annihilation of the deadly pandemic.

2. Formulation of system optimal control problem

In this section, we focus on defining the problem statement for our model, formulation of an optimal control problem and analysis of the mathematical properties of the derived problem.

2.1 Problem statement and model derivation

We base the present study on our previous model [8], where designated dual bilinear control functions constituted by pair non-pharmaceutical control functions (face masks and social distancing) and pair pharmaceutical intervention func-

tions (hydroxyl-chloroquine—HCQ and Azithromycin—AZT) were initiated on an 8-Dimensional deterministic COVID-19 dynamic model for the possible mitigation of the disease viral load. Therefore, the present study seeks to utilize the aforementioned system following the transformation of the basic model to an optimal control model. In that study, the spread of COVID-19 was considered from human-to human population of size $N(t)$ and then sub-divided into 8 sub-populations, which include: S_p - susceptible population to COVID-19 virus, X_p - exposed population, A_u - unaware asymptotic infectious population, I_a - aware infective population, I_s - isolated infectious population, S_s - super-spreaders infectious population, H_i - hospitalized infectious population and R_p - COVID-19 recovered population. The epidemiological equations of the model were derived as:

$$\begin{aligned}
\frac{dS_p}{dt} &= b_p + \sigma_1 X_p + \sigma_2 R_p - \beta_i(\hat{N})S_p - \mu S_p,\\
\frac{dX_p}{dt} &= \beta_i(\hat{N})S_p - (1-u_1)\lambda X_p - (\mu+\sigma_1)X_p,\\
\frac{dA_u}{dt} &= (1-u_1)\lambda X_p - (1-u_2)k\theta A_u - (1-a_1)(1-a_2)\varphi_1 A_u - (\mu+\alpha_1+\varphi_2)A_u,\\
\frac{dI_a}{dt} &= (1-u_2)k\theta A_u - [(1-a_1)(1-a_2)\rho_2 + a_1\tau_1\rho_1 + (1-\rho_1-\rho_2)]I_a - (\mu+\alpha_2)I_a,\\
\frac{dI_s}{dt} &= a_1\tau_1\rho_1 I_a + a_1\tau_2\gamma_s S_s - [(1-a_1)(1-a_2)\delta_h]I_s - (\mu+\alpha_4+\eta_2)I_s,\\
\frac{dS_s}{dt} &= (1-\rho_1-\rho_2)I_a + \varphi_2 A_u - a_1\tau_2\gamma_s S_s - (\mu+\alpha_5+\eta_3)S_s,\\
\frac{dH_i}{dt} &= (1-a_1)(1-a_2)[\varphi_1 A_u + \rho_2 I_a + \delta_h I_s] - (\mu+\alpha_3+\eta_1)H_i,\\
\frac{dR_p}{dt} &= \eta_1 H_i + \eta_2 I_s + \eta_3 S_s - (\mu+\sigma_2)R_p,
\end{aligned} \tag{1}$$

with initial conditions $S_p(t_0)>0,\quad X_p(t_0)>0,\quad A_u(t_0)>0,\quad I_a(t_0)>0,\quad I_s(t_0)>0,\quad S_s(t_0)>0,\quad H_i(t_0)>0,$ $R_p(t_0)>0$ for all $t=t_0$. Here, the system force of infection denoted by $\beta_i(\hat{N})=\beta_i(X_p,A_u,I_a,S_s,H_i)$ is given by

$$\beta_i(\hat{N}) = (1-u_1-u_2)\left[\frac{\beta_1 c_1 X_p + \beta_2 c_2 A_u + \beta_3 c_3 I_a + \beta_4 c_4 S_s + \beta_5 c_5 H_i}{N(t)}\right],\quad i=1,....,5 \tag{2}$$

where, $\hat{N} = X_p + A_u + I_a + S_s + H_i$ and

$$N(t) = S_p + X_p + A_u + I_a + I_s + S_s + H_i + R_p = 1. \tag{3}$$

Now, since interest is that of an optimal control, then for simplicity, we redefined the study control functions uniquely by choosing $q_{i=1,..,4}$ to represent the system dual bilinear control functions i.e. $q_{i=1,2}=u_{i=1,2}$ and $q_{i=3,4}=a_{i=1,2}$. Therefore, we redefined eq. (1) using $q_{i=1,..,4}$ and with the assumption that control functions $q_i>0$ is a function of time variation and having antiviral effect on aerosol viral load production [19]. That is, eq. (1) together with eq. (2) becomes

$$\begin{aligned}
\frac{dS_p}{dt} &= b_p + \sigma_1 X_p(t) + \sigma_2 R_p(t) - \beta_i(\hat{N})S_p(t) - \mu S_p(t),\\
\frac{dX_p}{dt} &= \beta_i(\hat{N})S_p(t) - (1-q_1)\lambda X_p(t) - (\mu+\sigma_1)X_p(t),\\
\frac{dA_u}{dt} &= (1-q_1)\lambda X_p(t) - (1-q_2)k\theta A_u(t) - (1-q_3)(1-q_4)\varphi_1 A_u(t) - (\mu+\alpha_1+\varphi_2)A_u(t),\\
\frac{dI_a}{dt} &= (1-q_2)k\theta A_u(t) - [(1-q_3)(1-q_4)\rho_2 + q_3\tau_1\rho_1 + (1-\rho_1-\rho_2)]I_a(t) - (\mu+\alpha_2)I_a(t),
\end{aligned}$$

$$\frac{dI_s}{dt} = q_3\tau_1\rho_1 I_a(t) + q_3\tau_2\gamma_s S_s(t) - [(1-q_3)(1-q_4)\delta_h]I_s(t) - (\mu+\alpha_4+\eta_2)I_s(t),$$

$$\frac{dS_s}{dt} = (1-\rho_1-\rho_2)I_a(t) + \varphi_2 A_u(t) - q_3\tau_2\gamma_s S_s(t) - (\mu+\alpha_5+\eta_3)S_s(t), \tag{4}$$

$$\frac{dH_i}{dt} = (1-q_3)(1-q_4)[\varphi_1 A_u(t) + \rho_2 I_a(t) + \delta_h I_s(t)] - (\mu+\alpha_3+\eta_1)H_i(t),$$

$$\frac{dR_p}{dt} = \eta_1 H_i(t) + \eta_2 I_s(t) + \eta_3 S_s(t) - (\mu+\sigma_2)R_p(t),$$

where initial conditions $N_i(t) \geq 0$ for all $t = t_0$, $i = 1,....,8$ with

$$\beta_i(\hat{N}) = (1-q_1-q_2)\left[\frac{\beta_1 c_1 X_p(t) + \beta_2 c_2 A_u(t) + \beta_3 c_3 I_a(t) + \beta_4 c_4 S_s(t) + \beta_5 c_5 H_i(t)}{N(t)}\right], \quad i = 1,....,5. \tag{5}$$

Thus, given eq. (5), model (4) represents a typical optimal control equation for COVID-19 with time dependent onset treatment. For brevity, the description of model terms, properties of system invariant region and positivity of solutions are omitted, since there are similar to those established by [8]. Since our model is time dependent, the dynamical flow-chart is as depicted by Fig. 1 below:

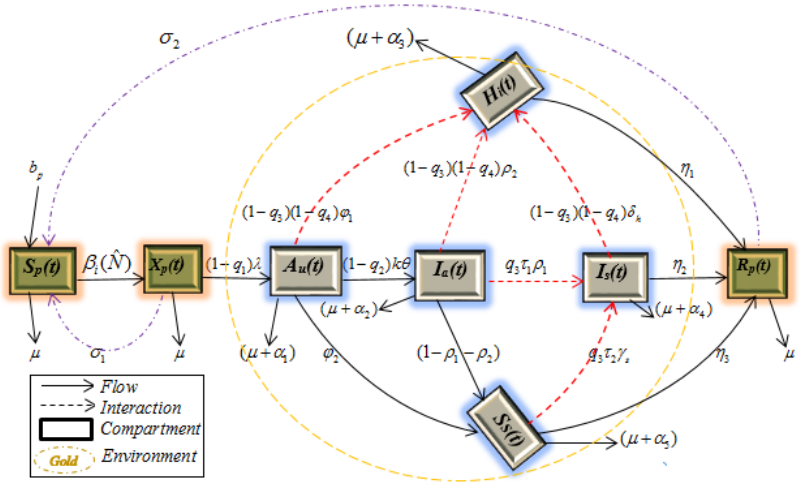

Figure 1. COVID-19 dynamic flow-chart with defined dual-bilinear control functions.

2.2 Optimal control problem for COVID-19 pandemic

In this subsection, using system (4) and Fig. 1, we present the process and derivation of an optimal control problem. Our intense is to enhance our previous model [8] by accounting for the maximization of the system performance index in terms of inclined maximal susceptible population, recovered population and at minimal control functions using model initial conditions. That is, given the control measures, we investigate the optimal levels required to minimize the spread of COVID-19 aerosol viral load at minimized systemic cost $q_{i=1,...,4}$. Achieving this goal, we consider in addition to the assumptions of model [8], the fact that study control functions are chosen as measurable functions defined as bounded Lebesgue integrable and satisfying fixed intervals i.e., $0 \leq a_i \leq q_i(t) \leq b_i < 1$ for all $i = 1,...,4$.

Remark 1

The basic assumption of this study follows from the fact that treatment duration is not infinite due to hazardous side effects and most therapies has terminal length period [20].

On critical analysis of model (4), we observe that aerosol viral load production under control functions q_1, q_2 is $\phi\beta_i(\hat{N})$, where $\phi = (1-q_1-q_2)$. Moreso, if $(q_3+q_4) = 1$, then annihilation of infection is 100% efficacious. Otherwise, no annihilation for all $(q_3+q_4) = 0$. Similarly, if controls (q_1+q_2) represent efficacy of face masking and social distancing in blocking new infection transmission, then the infection rate in the presence of q_1 and q_2 is evidently given by $\phi\beta_i(\hat{N})$

[21]. Therefore, the optimality problem that maximizes system (4) is defined by the objective functional

$$J(q_i)\max\int_{t_0}^{t_f}\left\{S_p(t)+R_p(t)-\left(\frac{1}{2}\sum_{i=1}^{4}Z_i(q_i(t))^2\right)\right\}dt, \tag{6}$$

subject to system (4) as constraints with treatment time limit $t\in[t_0,t_f]$. Clearly, eq. (6) is characterized by positive constants $Z_i\geq 0$ for all $i=1,..,4$. The quantity Z_i represents optimal weight factors defined on cost-benefits and which linearized the non-linear benefit on cost functional. The term $q_i(t)$ denotes cost of treatment (systemic cost) on control functions. Furthermore, the quadratic function $(q_i(t))^2$ reflects the severity of side-effect of control functions [22]. That is, the system objective functional is well-posed and which implies that we seek an optimal controls q_i^*, $i=1,..,4$ defined by

$$J(q_i^*)=\max_{0\leq q_i<1}\{J(q_i):q_i\in\pi\},\ i=1,..,4, \tag{7}$$

where $\pi=\left\{q_i^*\setminus q_i^*\right.$ is Lebesgue-measurable, $0\leq a_i\leq q_i(t)\leq b_i<1$, $\left.t\in[t_0,t_f],i=1,..,4\right\}$ a control set [23, 24].

Thus, the present approach is essential in the sense that, following the non-eradication of COVID-19 under dual-bilinear control functions studied using global stability analysis theory, the study proposes the methodological application of optimal treatment technique using similar dual-bilinear control functions and investigated using classical method of Pontryagin's maximum principle with the incorporation of the method of Hessian matrix in the system analysis.

3. Mathematical analysis of optimal controls

In this section, we attempt to establish the mathematical characterization associated with optimal controls and the existence of optimal controls.

3.1 Characterization of optimal controls

Here, we describe and analyze the optimal controls characterization as a necessary condition for the establishment of the existence of optimal controls for the system. We initiate this action by exploring the Pontryagin's maximum principle as had been done by [25] to determine our optimal controls q_i^*, $i=1,..,4$. That is, from eq. (6) and system (4), the Hamiltonian argument defined by the Lagrangian (L) is given by

$$\begin{aligned}L=L\left(t,S_p,X_p,A_u,I_a,I_s,S_s,H_i,R_p,q_i,\zeta_i\right)=S_p(t)+R_p(t)-\left(\frac{1}{2}\sum_{i=1}^{4}Z_i(q_i(t)^2)\right)+\sum_{i=1}^{8}\zeta_i f_i\\ +v_{11}(t)(b_1-q_1)+v_{12}(t)(q_1-a_1)+v_{21}(t)(b_2-q_2)\\ +v_{22}(t)(q_2-a_2)+w_{11}(t)(a_3-q_3)+w_{12}(t)(q_3-a_3)\\ +w_{21}(t)(b_4-q_4)+w_{22}(t)(q_4-a_4)\end{aligned}, \tag{8}$$

where $v_{11}(t),v_{12}(t),.....,w_{22}(t)\geq 0$ are penalty multipliers satisfying

$$\begin{aligned}v_{11}(t)(b_1-q_1)=0, v_{12}(t)(q_1-a_1)=0 \text{ at optimal } q_1^*\\ v_{21}(t)(b_2-q_2)=0, v_{22}(t)(q_2-a_2)=0 \text{ at optimal } q_2^*\\ w_{11}(t)(a_3-q_3)=0, w_{12}(t)(q_3-a_3)=0 \text{ at optimal } q_3^*\\ w_{21}(t)(b_4-q_4)=0, w_{22}(t)(q_4-a_4)=0 \text{ at optimal } q_4^*,\end{aligned}$$

for all $q_i\in[0,1], i=1,..,4$. From eq. (8), the functions $\zeta_i(t), i=1,...,8$ are the model adjoint variables, which determine the adjoint system with f_i representing the right-hand side of system (4). Then, we shall consider all possible values for the controls including those on the boundary $0\leq q_i^*\leq 1$ for all $i=1,..,4$.

i. Consider the set $\{t\setminus 0<q_i^*(t)<1\}:(v_{i,j}(t),w_{i,j})=0$ for all $i,j=1,2$. The Pontryagin's maximum principle state that unconstrained optimal control q_i^*, $i=1,..,4$ satisfies

$$\frac{\partial L}{\partial q_i^*} = 0 \text{ , } i = 1,..,4 \text{ .}$$

So, we find $\frac{\partial L}{\partial q_i^*}$ and solve for q_i^* by setting the partial derivatives of L equal to zero. Thus,

$$\frac{\partial L}{\partial q_1^*} = -Z_1 q_1^* + \zeta_2(\lambda X_p(t)) - \zeta_3(\lambda X_p(t)) - v_{11}(t) + v_{12}(t) = 0 \quad \text{at } q_1^*,$$

$$\frac{\partial L}{\partial q_2^*} = -Z_2 q_2^* + \zeta_3(k\theta A_u(t)) - \zeta_4(k\theta A_u(t)) - v_{21}(t) + v_{22}(t) = 0 \quad \text{at } q_2^*,$$

$$\begin{aligned}\frac{\partial L}{\partial q_3^*} &= -Z_3 q_3^* + \zeta_3(\varphi_1 A_u(t)) + \zeta_4(\rho_2 - \tau_1\rho_1) I_a(t) + \zeta_5[\tau_1\rho_1 I_a(t) \\ &+ \tau_2\gamma_s S_s(t) + \delta_h I_s(t)] - \zeta_6(\tau_2\gamma_s S_s(t)) \\ &\zeta_7[\varphi_1 A_u(t) + \rho_2 I_a(t) + \delta_h I_s(t)] - w_{11}(t) + w_{12}(t) = 0 \quad \text{at } q_3^*\end{aligned}$$

$$\begin{aligned}\frac{\partial L}{\partial q_4^*} &= -Z_4 q_4^* + \zeta_3(\varphi_1 A_u(t)) + \zeta_4(\rho_2 I_a(t)) + \zeta_5(\delta_h I_s(t)) - \zeta_7[\varphi_1 A_u(t) \\ &+ \rho_2 I_a(t) + \delta_h I_s(t)] - w_{21}(t) + w_{22}(t) = 0 \quad \text{at } q_4^*.\end{aligned}$$

Then, solving for q_i^*, $i = 1,..,4$ for all $v_{ij} = 0$ and $w_{ij} = 0$, we have

$$q_1^*(t) = \frac{1}{Z_1}\left\{\zeta_2(\lambda X_p(t)) - \zeta_3(\lambda X_p(t))\right\},$$

$$q_2^*(t) = \frac{1}{Z_2}\left\{\zeta_3(k\theta A_u(t)) - \zeta_4(k\theta A_u(t))\right\},$$

$$q_3^*(t) = \frac{1}{Z_3}\left\{\begin{matrix}\zeta_3(\varphi_1 A_u(t)) + \zeta_4(\rho_2 - \tau_1\rho_1) I_a(t) + \zeta_5[\tau_1\rho_1 I_a(t) + \tau_2\gamma_s S_s(t) + \delta_h I_s(t)] \\ -\zeta_6(\tau_2\gamma_s S_s(t)) - \zeta_7[\varphi_1 A_u(t) + \rho_2 I_a(t) + \delta_h I_s(t)]\end{matrix}\right\}$$

and

$$q_4^*(t) = \frac{1}{Z_4}\left\{\zeta_3(\varphi_1 A_u(t)) + \zeta_4(\rho_2 I_a(t)) + \zeta_5(\delta_h I_s(t)) - \zeta_7[\varphi_1 A_u(t) + \rho_2 I_a(t) + \delta_h I_s(t)]\right\}.$$

Furthermore, we consider the characterization at boundaries for $q_i^* = 0$ and $q_i^* = 1$ for all $i = 1,..,4$ as well as non-boundary cases.

ii. Consider the set $\{t \setminus 0 < q_i^*(t) = 0, \mathrm{i} = 1,..,4\} : v_{i,j} \geq 0, w_{i,j} \geq 0, v_{i2} = 0, w_{i2} = 0, i, j = 1$. Then, from the definition of the optimal controls, we have

$$0 = \frac{\zeta_2(\lambda X_p(t)) - \zeta_3(\lambda X_p(t)) - v_{1j}}{Z_1}.$$

Since $v_{1j} \geq 0$, we have

$$\frac{\zeta_2(\lambda X_p(t)) - \zeta_3(\lambda X_p(t))}{Z_1} \leq 0.$$

To ensure that q_1^* is non-negative, [26] had used the notation $s^+ = \max\{s, 0\}$ to redefine similar functions as q_i^*. Therefore,

$$q_1^*(t) = \left(\frac{\zeta_2(\lambda X_p(t)) - \zeta_3(\lambda X_p(t))}{Z_1}\right)^+.$$

Similarly,

$$q_2^*(t)=\left(\frac{\zeta_3(k\theta A_u(t))-\zeta_4(k\theta A_u(t))}{Z_2}\right)^+,$$

$$q_3^*(t)=\left(\begin{array}{l}\zeta_3(\varphi_1 A_u(t))+\zeta_4(\rho_2-\tau_1\rho_1)I_a(t)+\zeta_5[\tau_1\rho_1 I_a(t)+\tau_2\gamma_s S_s(t)+\delta_h I_s(t)]\\ -\zeta_6(\tau_2\gamma_s S_s(t))-\zeta_7[\varphi_1 A_u(t)+\rho_2 I_a(t)+\delta_h I_s(t)]\\ \hline Z_3\end{array}\right)^+$$

and

$$q_4^*(t)=\left(\frac{\zeta_3(\varphi_1 A_u(t))+\zeta_4(\rho_2 I_a(t))+\zeta_5(\delta_h I_s(t))-\zeta_7[\varphi_1 A_u(t)+\rho_2 I_a(t)+\delta_h I_s(t)]}{Z_4}\right)^+.$$

iii. The case for the set $\{t\setminus 0<q_i^*(t)=1,\mathrm{i}=1,..,4\}: v_{i,1}=0, w_{2,j}=0, v_{2j}=0, w_{2j}=0$ for all $i,j=2$. The optimal controls are derived as follows:

$$1=\frac{\zeta_2(\lambda X_p(t))-\zeta_3(\lambda X_p(t))+v_{2j}}{Z_1},$$

which implies that

$$0\le v_{2j}=\zeta_2(\lambda X_p(t))-\zeta_3(\lambda X_p(t))-Z_1.$$

Therefore,

$$q_1^*(t)=\left(\frac{\zeta_2(\lambda X_p(t))-\zeta_3(\lambda X_p(t))}{Z_1}\right)\ge 1.$$

Similarly,

$$q_2^*(t)=\left(\frac{\zeta_3(k\theta A_u(t))-\zeta_4(k\theta A_u(t))}{Z_2}\right)\ge 1,$$

$$q_3^*(t)=\left(\begin{array}{l}\zeta_3(\varphi_1 A_u(t))+\zeta_4(\rho_2-\tau_1\rho_1)I_a(t)+\zeta_5[\tau_1\rho_1 I_a(t)+\tau_2\gamma_s S_s(t)+\delta_h I_s(t)]\\ -\zeta_6(\tau_2\gamma_s S_s(t))-\zeta_7[\varphi_1 A_u(t)+\rho_2 I_a(t)+\delta_h I_s(t)]\\ \hline Z_3\end{array}\right)\ge 1$$

and

$$q_4^*(t)=\left(\frac{\zeta_3(\varphi_1 A_u(t))+\zeta_4(\rho_2 I_a(t))+\zeta_5(\delta_h I_s(t))-\zeta_7[\varphi_1 A_u(t)+\rho_2 I_a(t)+\delta_h I_s(t)]}{Z_4}\right)\ge 1.$$

Thus, the characterization for the optimal controls is complete by combining the three cases for $q_i^*(t)$ and compatibly defined as by the following proposition.

Proposition 1

The optimal controls for the optimality problem of system (4) with limits bounds $0\le a_i\le q_1^*\le b_i<1$ for all $i=1,...,4$, is completely characterized by

$$q_1^*(t)=\min\left\{\max\left\{a_1,\left(\frac{\zeta_2(\lambda X_p(t))-\zeta_3(\lambda X_p(t))}{Z_1}\right)\right\}^+,b_1\right\}, \tag{9}$$

$$q_2^*(t)=\min\left\{\max\left\{a_3,\left(\frac{\zeta_3(k\theta A_u(t))-\zeta_4(k\theta A_u(t))}{Z_2}\right)\right\}^+,b_3\right\}, \tag{10}$$

$$q_3^*(t)=\min\left\{\max\left\{a_2,\left(\frac{\begin{array}{l}\zeta_3(\varphi_1A_u(t))+\zeta_4(\rho_2-\tau_1\rho_1)I_a(t)+\zeta_5[\tau_1\rho_1I_a(t)+\tau_2\gamma_sS_s(t)+\delta_hI_s(t)]\\-\zeta_6(\tau_2\gamma_sS_s(t))-\zeta_7[\varphi_1A_u(t)+\rho_2I_a(t)+\delta_hI_s(t)]\end{array}}{Z_3}\right)^+,b_2\right\}\right\} \tag{11}$$

and

$$q_4^*(t)=\min\left\{\max\left\{a_4,\left(\frac{\zeta_3(\varphi_1A_u(t))+\zeta_4(\rho_2I_a(t))+\zeta_5(\delta_hI_s(t))-\zeta_7[\varphi_1A_u(t)+\rho_2I_a(t)+\delta_hI_s(t)]}{Z_4}\right)^+,b_4\right\}\right\}. \tag{12}$$

Remark 2

Unlike other transmittable diseases, the optimal controls for standard COVID-19 model are concurrently defined by both the system circulating asymptomatic and symptomatic infectious state variables and their corresponding adjoint variables [27].

3.2 Existence of optimal controls for COVID-19

The boundedness of solutions for system (4) in a finite time interval is used to prove the existence of system optimal controls. We prove this by using the fact that supersolutions $\overline{S}_p,\overline{X}_p,\overline{A}_u,\overline{I}_a,\overline{I}_s,\overline{S}_s,\overline{H}_i$ and $\overline{R}_p$ satisfying system (4) are bounded on a finite time interval. Thus, existence of system optimal controls can be obtained using the following theorem.

Theorem 1

Consider the control problem with system (4). Then, there exists $\vec{q}^*=\{q_1^*,q_2^*,q_3^*,q_4^*\}\in\pi$ such that the maximization of the objective functional is given by

$$J(q_i^*)=\max_{q_i\in\pi}J(q_i),\quad i-1,...,4.$$

Proof

We invoke existence results from [21, 24, 26], which requires that we check for the following properties:

(C_1) The set of controls $q_i(t),i=1,..,4$ are Lebesgue-integrable with non-empty corresponding state variables.

(C_2) The admissible control set π, is convex and closed.

(C_3) The RHS of the state system is bounded by linear functions of $q_i(t)$ with coefficients that depend on the state variables and on proposition1.

(C_4) The integrand of the objective functional is concave on π.

(C_5) There exists constants $c_1,c_2>0$ and $\sigma>1$ such that the integrand

$$L\left(S_p,R_p,q_i\right)\le c_2-c_1\left(\sum_{i=1}^{4}|q_i|^2\right)^{\sigma/2},\quad i=1,..,4.$$

Then, from existing results, we see that the boundedness of the state system (4) with control eqs (9)-(12) ensures the existence of solutions, which can be deduce that the set of controls and corresponding state variables are non-empty, thus, satisfying (C_1). By definition, the control set is then convex and closed, which ensure condition (C_2).

Furthermore, since the system is characterized by dual-bilinear in $q_i(t),i=1,..,4$, the right-hand side of model (4) verifies condition (C_3) for the fact that the solutions are bounded. Note that for condition (C_4), we apply the Hessian matrix for J as follows:

$$\Upsilon_J=\begin{pmatrix}-Z_1&0&0&0\\0&-Z_2&0&0\\0&0&-Z_3&0\\0&0&0&-Z_4\end{pmatrix}$$

with determinant

$$\det(\Upsilon_J)=[(-Z_1)(-Z_2)(-Z_3)(-Z_4)]\ge 0,\quad \forall q_i\in\pi.$$

Then, J is concave on π. Moreso, from condition (C_5), we have

$$L\left(S_p, R_p, q_i\right) \le c_2 - c_1\left(\sum_{i=1}^{4} |\, q_i \,|^2\right)$$

with c_2 depending on the upper-bound on S_p, R_p and $c_1 = \min\sum_{i=1}^{4}\left(\frac{Z_i}{2}\right) > 0$. Hence, we conclude that there exists optimal controls $q_{i=1,..,4} \in \pi$ such that $J(q_i^*) = \max_{(q_i)\in\pi} J(q_i), i = 1,..,4$, which complete the proof.

4. Model Optimality System and Uniqueness

Following the transformation of system model to an optimal control problem and the investigation of the existence of model optimal controls, we devote this section to the derivation of model optimality system and its uniqueness.

4.1 Optimality system for COVID-19 model

Optimality system is an approach that defines the biological behavior of system state variables as well as the determination of system growth and/or clearance rate. Notably, our study is that of bilinear maximization of designated state variables (S_p, R_p) following methodological application of dual bilinear control functions. Then, in deriving the model optimality system as a vital component of optimal control problem, we explore classical Pontryagin's maximum principle [28].

Definition 1

Optimality system consists of model state system couple with the adjoint system with initial and transversality conditions together with derived optimal controls.

By definition 1, we note that the system with initial conditions as well as optimal controls has been derived. That is, we require next, a well-posed adjoint system and transversality conditions for the complete derivation of our required optimality system. We know from [26] that the adjoint system is given by

$$\frac{d\zeta_i}{dt} = -\frac{\partial L}{\partial f_i},$$

where $f_{i-1,...,8}$ are the state variables. Now, suppose we consider a maximization problem of the type:

$$\max_{(q_i)\in\pi} J(q_i) = F(S_p(t) + \int_{t_0}^{t_f} g_0(S_p, q_i))dv, \quad i = 1,..,4,$$

subject to the system $\frac{dS_p}{dt} = g(t, S_p, q_i)$ such that $x(S_p) \in k(x(S_p))$. Then, the following transversality conditions on the adjoint variables holds:

$$\zeta_i(t) = \overline{\upsilon} F(x(S_p(t))) + \sum_{i=1}^{m} c_i k_i(S_p(t)). \tag{13}$$

From eq. (13), F denotes terminal cost. However, our model has no terminal cost index, so $F(x(S_p(t))) = 0$. We also note that our problem does not come with set target for the state variables. Rather, we look forward for a desired end result. That is, our last term is thus free, so the summation term is also zero. Therefore, the transversality condition for the adjoint variables is

$$\zeta_i(t) = 0, \quad i = 1,...,8. \tag{14}$$

The following theorem gives the required well-posed adjoint system for our optimality system.

Theorem 2

Given the system of system (4), let (q_i^*), $i = 1,...,4$ be the optimal controls with $S_p^*, X_p^*, A_u^*, I_a^*, I_s^*, S_s^*, H_i^*, R_p^*$ as system solutions. Then, there exists adjoint variables $\zeta_i(t) = 0$ for all $i = 1,...,8$ satisfying the equations

$$\zeta_1'(t) = -1\{\zeta_1(t)[-(1-q_1^*(t)-q_2^*(t))(\beta_1 c_1 X_p^*(t) + \beta_2 c_2 A_u^*(t) + \beta_3 c_3 I_a^*(t) + \beta_4 c_4 S_s^*(t) + \beta_5 c_5 H_i^*(t)) - \mu$$

$$\zeta_2(t)[(1-q_1^*(t)-q_2^*(t))(\beta_1 c_1 X_p^*(t) + \beta_2 c_2 A_u^*(t) + \beta_3 c_3 I_a^*(t) + \beta_4 c_4 S_s^*(t) + \beta_5 c_5 H_i^*(t))\},$$

$$\zeta_2'(t) = -1\begin{Bmatrix}\zeta_1(t)[\sigma_1 - (1-q_1^*(t)-q_2^*(t))\beta_1 c_1 S_p^*(t)] - \zeta_2(t)[(1-q_1^*(t)-q_2^*(t))\beta_1 c_1 S_p^*(t)\\ +(1-q_1^*(t))\lambda + (\mu+\sigma_1)] - \zeta_3(t)\lambda\end{Bmatrix},$$

$$\zeta_3'(t) = -1\begin{Bmatrix}\zeta_1(t)[-(1-q_1^*(t)-q_2^*(t))\beta_2 c_2 S_p^*(t)] - \zeta_3(t)[(1-q_2^*(t))k\theta + (1-q_4^*(t))\varphi_1 + (\mu+\alpha_1+\varphi_2)]\\ +\zeta_4(t)(1-q_2^*(t))k\theta + \zeta_6(t)\varphi_2 + \zeta_7(t)(1-q_3^*(t)((1-q_4^*(t))\varphi_1 H_i^*(t)\end{Bmatrix},$$

$$\zeta_4'(t) = -1\begin{Bmatrix}\zeta_1(t)[-(1-q_1^*(t)-q_2^*(t))\beta_3 c_3 S_p^*(t)] + \zeta_2(t)[(1-q_1^*(t)-q_2^*(t))\beta_3 c_3 S_p^*(t)]\\ -\zeta_4(t)[(1-q_3^*(t)((1-q_4^*(t))\rho_2 + q_3^*(t)\tau_1\rho_1 + (1-\rho_1-\rho) + (\mu+\alpha_2)]\\ +\zeta_5(t)q_3^*(t)\tau_1\rho_1 + \zeta_6(t)(1-\rho_1-\rho) + \zeta_7(t)(1-q_3^*(t)((1-q_4^*(t))\rho_2\end{Bmatrix},$$

$$\zeta_5'(t) = -1\left\{-\zeta_5(t)[\sigma_1 - (1-q_3^*(t))(1-q_4^*(t))\delta_h + (\mu+\alpha_4+\eta_2)] + \zeta_7[(t)[\sigma_1 - (1-q_3^*(t))(1-q_4^*(t))]\delta_h + \zeta_8(t)\eta_2\right\},$$

$$\zeta_6'(t) = -1\begin{Bmatrix}\zeta_1(t)[-(1-q_1^*(t)-q_2^*(t))\beta_4 c_4 S_p^*(t)] + \zeta_2(t)[(1-q_1^*(t)-q_2^*(t))\beta_4 c_4 S_p^*(t)]\\ +\zeta_5(t)[q_3^*(t)\tau_2\gamma_s] - \zeta_6(t)[q_3^*(t)\tau_2\gamma_s + (\mu+\alpha_5+\eta_3)] + \zeta_8(t)\eta_3\end{Bmatrix},$$

$$\zeta_7'(t) = -1\begin{Bmatrix}\zeta_1(t)[-(1-q_1^*(t)-q_2^*(t))\beta_4 c_5 S_p^*(t)] + \zeta_2(t)[(1-q_1^*(t)-q_2^*(t))\beta_5 c_5 S_p^*(t)]\\ -\zeta_7(t)(\mu+\alpha_5+\eta_3) + \zeta_8(t)\eta_1\end{Bmatrix}, \quad (15)$$

$$\zeta_8'(t) = -1\{\zeta_1(t)\sigma_2 + \zeta_8(t)(\mu+\sigma_2)\},$$

where $\zeta_i(t_f) = 0$ for all $i = 1,...,8$ are the transversality conditions with $q_i^*(t)$, $i = 1,...,4$ defined by proposition 1.

Proof

Invoking results of optimality systems from [19, 22, 28], we see that the transversality conditions and adjoint equations are derived from

$$\frac{d\zeta_i}{dt} = -\frac{\partial L}{\partial f_i}, \quad i = 1,...,8.$$

where $\frac{\partial L}{\partial f_i}$ is depicted by eq. (15). Then, finding the derivatives of ζ_i, we have

$$\begin{cases}\zeta_1'(t) = -\frac{\partial L}{\partial S_p}(t) & \zeta_1(t_f) = 0\\ \zeta_2'(t) = -\frac{\partial L}{\partial X_p}(t) & \zeta_2(t_f) = 0\\ \zeta_3'(t) = -\frac{\partial L}{\partial A_u}(t) & \zeta_3(t_f) = 0\\ \zeta_4'(t) = -\frac{\partial L}{\partial I_a}(t) & \zeta_4(t_f) = 0\\ \zeta_5'(t) = -\frac{\partial L}{\partial I_s}(t) & \zeta_5(t_f) = 0\\ \zeta_6'(t) = -\frac{\partial L}{\partial S_s}(t) & \zeta_6(t_f) = 0\\ \zeta_7'(t) = -\frac{\partial L}{\partial H_i}(t) & \zeta_7(t_f) = 0\\ \zeta_8'(t) = -\frac{\partial L}{\partial R_p}(t) & \zeta_8(t_f) = 0\end{cases} \quad (16)$$

Therefore, by definition 1, the required optimality system is obtained by the explicit combination of system (4) and eq. (16), upon substituting eqs (9)-(12) into system (4) and eq. (15) into eq. (16) to give

$$\frac{dS}{dt} = b_p + \sigma_1 X_p^*(t) + \sigma_2 R_p^*(t) - \frac{(1-q_1^*-q_2^*)}{N(t)}\begin{bmatrix}\beta_1 c_1 X_p^*(t) + \beta_2 c_2 I_a^*(t) + \beta_3 c_3 I_s^*(t)\\ +\beta_4 c_4 S_s^*(t) + \beta_5 c_5 H_i^*(t)\end{bmatrix} S_p^*(t) - \mu S_p^*(t),$$

$$\frac{dX}{dt} = \frac{(1-q_1^*-q_2^*)}{N(t)}\begin{bmatrix}\beta_1 c_1 X_p^*(t) + \beta_2 c_2 I_a^*(t) + \beta_3 c_3 I_s^*(t) + \beta_4 c_4 S_s^*(t)\\ +\beta_5 c_5 H_i^*(t)\end{bmatrix} S_p^*(t) - (1-q_1^*)\lambda X_p^*(t) - (\mu+\sigma_1) X_p^*(t),$$

$$\frac{dA_u}{dt} = (1-q_1^*)\lambda X_p^*(t) - (1-q_2^*)k\theta A_u^*(t) - (1-q_3^*)(1-q_4^*)\varphi_1 A_u^*(t) - (\mu+\alpha_1+\varphi_2)A_u^*(t),$$

$$\frac{dI_a}{dt} = (1-q_2^*)k\theta A_u^*(t) - [(1-q_3^*)(1-q_4^*)\rho_2 + q_3^*\tau_1\rho_1 + (1-\rho_1-\rho_2)]I_a^*(t) - (\mu+\alpha_2)I_a^*(t),$$

$$\frac{dI_s}{dt} = q_3^*\tau_1\rho_1 I_a^*(t) + q_3^*\tau_2\gamma_s S_s^*(t) - [(1-q_3^*)(1-q_4^*)\delta_h]I_s^*(t) - (\mu+\alpha_4+\eta_2)I_s^*(t),$$

$$\frac{dS_s}{dt} = (1-\rho_1-\rho_2)I_a^*(t) + \varphi_2 A_u^*(t) - q_3^*\tau_2\gamma_s S_s^*(t) - (\mu+\alpha_5+\eta_3)S_s^*(t),$$

$$\frac{dH_i}{dt} = (1-q_3^*)(1-q_4^*)[\varphi_1 A_u^*(t) + \rho_2 I_a^*(t) + \delta_h I_s^*(t)] - (\mu+\alpha_3+\eta_1)H_i^*(t),$$

$$\frac{dR_p}{dt} = \eta_1 H_i^*(t) + \eta_2 I_s^*(t) + \eta_3 S_s^*(t) - (\mu+\sigma_2)R_p^*(t),$$

$$\zeta_1'(t) = -1\Big\{\zeta_1(t)[-(1-q_1^*(t)-q_2^*(t))(\beta_1 c_1 X_p^*(t) + \beta_2 c_2 A_u^*(t) + \beta_3 c_3 I_a^*(t) + \beta_4 c_4 S_s^*(t) + \beta_5 c_5 H_i^*(t)) - \mu]$$

$$\zeta_2(t)[(1-q_1^*(t)-q_2^*(t))(\beta_1 c_1 X_p^*(t) + \beta_2 c_2 A_u^*(t) + \beta_3 c_3 I_a^*(t) + \beta_4 c_4 S_s^*(t) + \beta_5 c_5 H_i^*(t)]\Big\},$$

$$\zeta_2'(t) = -1\begin{Bmatrix}\zeta_1(t)[\sigma_1 - (1-q_1^*(t)-q_2^*(t))\beta_1 c_1 S_p^*(t)] - \zeta_2(t)[(1-q_1^*(t)-q_2^*(t))\beta_1 c_1 S_p^*(t)\\ +(1-q_1^*(t))\lambda + (\mu+\sigma_1)] - \zeta_3(t)\lambda\end{Bmatrix},$$

$$\zeta_3'(t) = -1\begin{Bmatrix}\zeta_1(t)[-(1-q_1^*(t)-q_2^*(t))\beta_2 c_2 S_p^*(t)] - \zeta_3(t)[(1-q_2^*(t))k\theta + (1-q_4^*(t))\varphi_1 + (\mu+\alpha_1+\varphi_2)]\\ +\zeta_4(t)(1-q_2^*(t))k\theta + \zeta_6(t)\varphi_2 + \zeta_7(t)(1-q_3^*(t)((1-q_4^*(t))\varphi_1 H_i^*(t)\end{Bmatrix},$$

$$\zeta_4'(t) = -1\begin{Bmatrix}\zeta_1(t)[-(1-q_1^*(t)-q_2^*(t))\beta_3 c_3 S_p^*(t)] + \zeta_2(t)[(1-q_1^*(t)-q_2^*(t))\beta_3 c_3 S_p^*(t)]\\ -\zeta_4(t)[(1-q_3^*(t)((1-q_4^*(t))\rho_2 + q_3^*(t)\tau_1\rho_1 + (1-\rho_1-\rho) + (\mu+\alpha_2)]\\ +\zeta_5(t)q_3^*(t)\tau_1\rho_1 + \zeta_6(t)(1-\rho_1-\rho) + \zeta_7(t)(1-q_3^*(t)((1-q_4^*(t))\rho_2\end{Bmatrix},$$

$$\zeta_5'(t) = -1\Big\{-\zeta_5(t)[\sigma_1 - (1-q_3^*(t))(1-q_4^*(t))\delta_h + (\mu+\alpha_4+\eta_2)] + \zeta_7[(t)[\sigma_1 - (1-q_3^*(t))(1-q_4^*(t))]\delta_h + \zeta_8(t)\eta_2\Big\},$$

$$\zeta_6'(t) = -1\begin{Bmatrix}\zeta_1(t)[-(1-q_1^*(t)-q_2^*(t))\beta_4 c_4 S_p^*(t)] + \zeta_2(t)[(1-q_1^*(t)-q_2^*(t))\beta_4 c_4 S_p^*(t)]\\ +\zeta_5(t)[q_3^*(t)\tau_2\gamma_s] - \zeta_6(t)[q_3^*(t)\tau_2\gamma_s + (\mu+\alpha_5+\eta_3)] + \zeta_8(t)\eta_3\end{Bmatrix},$$

$$\zeta_7'(t) = -1\begin{Bmatrix}\zeta_1(t)[-(1-q_1^*(t)-q_2^*(t))\beta_4 c_5 S_p^*(t)] + \zeta_2(t)[(1-q_1^*(t)-q_2^*(t))\beta_5 c_5 S_p^*(t)]\\ -\zeta_7(t)(\mu+\alpha_5+\eta_3) + \zeta_8(t)\eta_1\end{Bmatrix},$$

$$\zeta_8'(t) = -1\{\zeta_1(t)\sigma_2 + \zeta_8(t)(\mu+\sigma_2\}, \tag{17}$$

with

$$q_1^*(t)=\min\left\{\max\left\{a_1,\left(\frac{\zeta_2(\lambda X_p^*(t))-\zeta_3(\lambda X_p^*(t))}{Z_1}\right)\right\}^+,b_1\right\},$$

$$q_2^*(t)=\min\left\{\max\left\{a_3,\left(\frac{\zeta_3(k\theta A_u^*(t))-\zeta_4(k\theta A_u^*(t))}{Z_2}\right)\right\}^+,b_3\right\},$$

$$q_3^*(t)=\min\left\{\max\left\{a_2,\left(\frac{\begin{array}{l}\zeta_3(\varphi_1 A_u^*(t))+\zeta_4(\rho_2-\tau_1\rho_1)I_a^*(t)+\zeta_5[\tau_1\rho_1 I_a^*(t)+\tau_2\gamma_s S_s^*(t)+\delta_h I_s^*(t)]\\ -\zeta_6(\tau_2\gamma_s S_s^*(t))-\zeta_7[\varphi_1 A_u^*(t)+\rho_2 I_a^*(t)+\delta_h I_s^*(t)]\end{array}}{Z_3}\right)\right\}^+,b_2\right\}$$

$$q_4^*(t)=\min\left\{\max\left\{a_4,\left(\frac{\zeta_3(\varphi_1 A_u^*(t))+\zeta_4(\rho_2 I_a^*(t))+\zeta_5(\delta_h I_s^*(t))-\zeta_7[\varphi_1 A_u^*(t)+\rho_2 I_a^*(t)+\delta_h I_s^*(t)]}{Z_4}\right)\right\}^+,b_4\right\}.$$

where $\zeta_i(t_f)=0$ for all $i=1,...,8$ are the transversality conditions and $N_i(0)=N_{(i)0}$, as state variables.

Finally, we investigate the uniqueness of optimality system for possibly small time interval.

4.2 Uniqueness of optimality system

We complete our theoretical predictions with the investigation of uniqueness of the model optimality system using the following lemma and theorem.

Lemma 1

Let $q^*=(q^*_{i=1,..,4})$ such that the function $q^*(b_p)=(\min(\max(b_p,a),b))$ is Lipschitz continuous in b_p, where $a<b$ are some fixed positive constants.

Theorem 3

For a typical infectious model (4), let the optimality system be given by eq. (17). Then, the bounded solutions of the optimality system are unique provided the upperbounds time interval t_f is sufficiently small.

Proof

We apply uniqueness of optimality system results from [20, 22, 27].

Let $(S_p,X_p,A_u,I_a,I_s,S_s,H_i,R_p,\zeta_i)$ and $(\bar{S}_p,\bar{X}_p,\bar{A}_u,\bar{I}_a,\bar{I}_s,\bar{S}_s,\bar{H}_i,\bar{R}_p,\bar{\zeta}_i)$ be two different solutions of the model optimality eq. (17), where $i=1,...,8$. Suppose we choose $\delta>0$ such that the values of the solutions are obtained by setting

$$S_p=g^{\delta t}e, X_p=g^{\delta t}f, A_u=g^{\delta t}h, I_a=g^{\delta t}l, I_s=g^{\delta t}j, S_s=g^{\delta t}k, H_i=g^{\delta t}m, R_p=g^{\delta t}n$$
$$\zeta_1=g^{\delta t}p,\zeta_2=g^{\delta t}q,\zeta_3=g^{\delta t}s,\zeta_4=g^{\delta t}t,\zeta_5=g^{\delta t}u,\zeta_6=g^{\delta t}w,\zeta_7=g^{\delta t}x,\zeta_8=g^{\delta t}v$$

and (18)

$$\bar{S}_p=g^{\delta t}\bar{e}, \bar{X}_p=g^{\delta t}\bar{f}, \bar{A}_u=g^{\delta t}\bar{h}, \bar{I}_a=g^{\delta t}\bar{l}, \bar{I}_s=g^{\delta t}\bar{j}, \bar{S}_s=g^{\delta t}\bar{k}, \bar{H}_i=g^{\delta t}\bar{m}, \bar{R}_p=g^{\delta t}\bar{n}$$
$$\bar{\zeta}_1=g^{\delta t}\bar{p},\bar{\zeta}_2=g^{\delta t}\bar{q},\bar{\zeta}_3=g^{\delta t}\bar{s},\bar{\zeta}_4=g^{\delta t}\bar{t},\bar{\zeta}_5=g^{\delta t}\bar{u},\bar{\zeta}_6=g^{\delta t}\bar{w},\bar{\zeta}_7=g^{\delta t}\bar{x},\bar{\zeta}_8=g^{\delta t}\bar{v}.$$

Furthermore, let $q_i^*(t)\ i=1,..,4$ be defined by eqs (9)-(12) of proposition 1 such that using eq. (18), the optimal controls becomes:

$$q_1^*(t)=\min\left\{\max\left\{a_1,\frac{1}{Z_1}\lambda(q-s)\right\}^+,b_1\right\},$$

$$q_2^*(t)=\min\left\{\max\left\{a_3,\frac{1}{Z_2}k\theta h(s-t)\right\}^+,b_3\right\},$$

$$q_3^*(t)=\min\left\{\max\left\{a_2,\frac{1}{Z_3}\left(\varphi_1 sh+(\rho_2-\tau_1\rho_1)(lt)+u(\tau_1\rho_1 l+\tau_2\gamma_s k+\delta_h j)-\tau_2\gamma_s(wk)\right)\right\}^+,b_2\right\},$$

$$q_4^*(t)=\min\left\{\max\left\{a_4,\frac{1}{Z_4}\left(\varphi_1(sh))+\rho_2(lt))+\delta_h(uj)-x(\varphi_1 h+\rho_2 l+\delta_h j)\right)\right\}^+,b_4\right\},$$

$$\bar{q}_1^*(t)=\min\left\{\max\left\{a_1,\frac{1}{Z_1}\lambda(\bar{q}-\bar{s})\right\}^+,b_1\right\},$$

$$\bar{q}_2^*(t)=\min\left\{\max\left\{a_3,\frac{1}{Z_2}k\theta(\bar{h}\bar{s}-\bar{h}\bar{t})\right\}^+,b_3\right\},$$

$$\bar{q}_3^*(t)=\min\left\{\max\left\{a_2,\frac{1}{Z_3}\left(\varphi_1(\bar{s}\bar{h})+(\rho_2-\tau_1\rho_1)(\bar{l}\bar{t})+\tau_1\rho_1(\bar{u}\bar{l})+\tau_2\gamma_s(\bar{u}\bar{k})+\delta_h(\bar{u}\bar{j})-\tau_2\gamma_s(\bar{w}\bar{k})\right)\right\}^+,b_2\right\}$$

and

$$\bar{q}_4^*(t)=\min\left\{\max\left\{a_4,\frac{1}{Z_4}\left(\varphi_1(\bar{s}\bar{h}))+\rho_2(\bar{l}\bar{t}))+\delta_h(\bar{u}\bar{j})-\varphi_1(\bar{x}\bar{h})-\rho_2(\bar{x}\bar{l})-\delta_h(\bar{x}\bar{j})\right)\right\}^+,b_4\right\}.$$

Also, substituting eq.(18) into the ODEs of eq.(17), we have

$$e'+\delta e=b_p+\sigma_1 g^{\delta t}f+\sigma_2 g^{\delta t}n-\frac{(1-q_1^*-q_2^*)}{N(t)}\begin{bmatrix}\beta_1c_1g^{\delta t}f+\beta_2c_2g^{\delta t}h+\beta_3c_3g^{\delta t}l\\+\beta_4c_4g^{\delta t}k+\beta_5c_5g^{\delta t}m\end{bmatrix}g^{\delta t}e-\mu g^{\delta t}e,$$

$$f'+\delta f=\frac{(1-q_1^*-q_2^*)}{N(t)}\begin{bmatrix}\beta_1c_1g^{\delta t}f+\beta_2c_2g^{\delta t}h+\beta_3c_3g^{\delta t}l\\+\beta_4c_4g^{\delta t}k+\beta_5c_5g^{\delta t}m\end{bmatrix}g^{\delta t}e-(1-q_1^*)\lambda g^{\delta t}f-(\mu+\sigma_1)g^{\delta t}f,$$

$$h'+\delta h=(1-q_1^*)\lambda g^{\delta t}f-(1-q_2^*)k\theta g^{\delta t}h-(1-q_3^*)(1-q_4^*)\varphi_1 g^{\delta t}h-(\mu+\alpha_1+\varphi_2)g^{\delta t}h,$$

$$l'+\delta l=(1-q_2^*)k\theta g^{\delta t}h-[(1-q_3^*)(1-q_4^*)\rho_2+q_3^*\tau_1\rho_1+(1-\rho_1-\rho_2)]g^{\delta t}l-(\mu+\alpha_2)g^{\delta t}l,$$

$$j'+\delta j=q_3^*\tau_1\rho_1 g^{\delta t}l+q_3^*\tau_2\gamma_s g^{\delta t}k-[(1-q_3^*)(1-q_4^*)\delta_h]g^{\delta t}j-(\mu+\alpha_4+\eta_2)g^{\delta t}j,$$

$$k'+\delta k=(1-\rho_1-\rho_2)g^{\delta t}j+\varphi_2 g^{\delta t}h-q_3^*\tau_2\gamma_s g^{\delta t}k-(\mu+\alpha_5+\eta_3)g^{\delta t}k,$$

$$m'+\delta m=(1-q_3^*)(1-q_4^*)[\varphi_1 g^{\delta t}h+\rho_2 g^{\delta t}l+\delta_h g^{\delta t}j]-(\mu+\alpha_3+\eta_1)g^{\delta t}m,$$

$$n'+\delta n=\eta_1 g^{\delta t}m+\eta_2 g^{\delta t}j+\eta_3 g^{\delta t}k-(\mu+\sigma_2)g^{\delta t}n,$$

$$\zeta_1'+\delta\zeta_1=-1\Big\{\zeta_1(t)[-(1-q_1^*(t)-q_2^*(t))(\beta_1c_1g^{\delta t}f+\beta_2c_2g^{\delta t}h+\beta_3c_3g^{\delta t}l+\beta_4c_4g^{\delta t}k+\beta_5c_5g^{\delta t}m-\mu)]$$

$$\zeta_2(t)[(1-q_1^*(t)-q_2^*(t))(\beta_1c_1g^{\delta t}f+\beta_2c_2g^{\delta t}h+\beta_3c_3g^{\delta t}l+\beta_4c_4g^{\delta t}k+\beta_5c_5g^{\delta t}m]\Big\},$$

$$\zeta_2'+\delta\zeta_2=-1\begin{Bmatrix}\zeta_1(t)[\sigma_1-(1-q_1^*(t)-q_2^*(t))\beta_1c_1g^{\delta t}e]-\zeta_2(t)[(1-q_1^*(t)-q_2^*(t))\beta_1c_1g^{\delta t}e\\+(1-q_1^*(t))\lambda+(\mu+\sigma_1)]-\zeta_3(t)\lambda\end{Bmatrix},$$

$$\zeta_3'+\delta\zeta_3=-1\begin{Bmatrix}\zeta_1(t)[-(1-q_1^*(t)-q_2^*(t))\beta_2c_2g^{\delta t}e]-\zeta_3(t)[(1-q_2^*(t))k\theta+(1-q_4^*(t))\varphi_1+(\mu+\alpha_1+\varphi_2)]\\+\zeta_4(t)(1-q_2^*(t))k\theta+\zeta_6(t)\varphi_2+\zeta_7(t)(1-q_3^*(t)((1-q_4^*(t))\varphi_1 g^{\delta t}m\end{Bmatrix},$$

$$\zeta_4' + \delta\zeta_4 = -1\begin{Bmatrix}\zeta_1(t)[-(1-q_1^*(t)-q_2^*(t))\beta_3 c_3 g^{\delta t}e] + \zeta_2(t)[(1-q_1^*(t)-q_2^*(t))\beta_3 c_3 g^{\delta t}e] \\ -\zeta_4(t)[(1-q_3^*(t)((1-q_4^*(t))\rho_2 + q_3^*(t)\tau_1\rho_1 + (1-\rho_1-\rho) + (\mu+\alpha_2)] \\ +\zeta_5(t)q_3^*(t)\tau_1\rho_1 + \zeta_6(t)(1-\rho_1-\rho) + \zeta_7(t)(1-q_3^*(t)((1-q_4^*(t))\rho_2\end{Bmatrix},$$

$$\zeta_5' + \delta\zeta_5 = -1\begin{Bmatrix}-\zeta_5(t)[\sigma_1 - (1-q_3^*(t))(1-q_4^*(t))\delta_h + (\mu+\alpha_4+\eta_2)] \\ +\zeta_7[(t)[\sigma_1 - (1-q_3^*(t))(1-q_4^*(t))]\delta_h + \zeta_8(t)\eta_2\end{Bmatrix},$$

$$\zeta_6' + \delta\zeta_6 = -1\begin{Bmatrix}\zeta_1(t)[-(1-q_1^*(t)-q_2^*(t))\beta_4 c_4 g^{\delta t}e] + \zeta_2(t)[(1-q_1^*(t)-q_2^*(t))\beta_4 c_4 g^{\delta t}e] \\ +\zeta_5(t)[q_3^*(t)\tau_2\gamma_s] - \zeta_6(t)[q_3^*(t)\tau_2\gamma_s + (\mu+\alpha_5+\eta_3)] + \zeta_8(t)\eta_3\end{Bmatrix},$$

$$\zeta_7' + \delta\zeta_7 = -1\begin{Bmatrix}\zeta_1(t)[-(1-q_1^*(t)-q_2^*(t))\beta_4 c_5 g^{\delta t}e] + \zeta_2(t)[(1-q_1^*(t)-q_2^*(t))\beta_5 c_5 g^{\delta t}e] \\ -\zeta_7(t)(\mu+\alpha_5+\eta_3) + \zeta_8(t)\eta_1\end{Bmatrix},$$

$$\zeta_8' + \delta\zeta_8 = -1\{\zeta_1(t)\sigma_2 + \zeta_8(t)(\mu+\sigma_2)\}.$$

We then perform the process of subtracting the state solutions $\overline{S}_p$ from S_p, $\overline{X}_p$ from X_p,……, ζ_8' from ζ_8 and then multiply the results obtained by appropriate difference of functions and then integrate from t_0 to t_f. The final resulting sixteen integral equations are summed and the uniqueness derived by estimate approach. Thus, guided by lemma 1, we have

$$\left|q_1^*(t) - \overline{q}_1^*(t)\right| \le \frac{1}{Z_1}\left|\lambda[(q-s) - (\overline{q}+\overline{s})]\right|,$$

$$\left|q_2^*(t) - \overline{q}_2^*(t)\right| \le \frac{1}{Z_2}\left|\theta k[hs(ht) - hs(\overline{ht})]\right|,$$

$$\left|q_3^*(t) - \overline{q}_3^*(t)\right| \le \frac{1}{Z_3}\begin{vmatrix}\varphi_1(hs-\overline{sh}) - (\rho_2-\tau_1\rho_1)(tl-\overline{tl}) - \tau_1\rho_1(ul-\overline{ul}) \\ -\tau_2\gamma_s(uk+\overline{uk}) - \delta_h(uj+\overline{uj}) - \tau_2\gamma_s(wk+\overline{wk})\end{vmatrix}$$

and

$$\left|q_4^*(t) - \overline{q}_4^*(t)\right| \le \frac{1}{Z_4}\begin{vmatrix}\varphi_1(hs-\overline{sh}) + \rho_2(tl-\overline{tl}) + \delta_h(uj+\overline{uj}) \\ -\rho_2\gamma_s(xl-\overline{xl}) - \delta_h(xj+\overline{xj})\end{vmatrix}.$$

Illustrating one case of the estimate approach on $\left|q_1^* - \overline{q}_1^*(t)\right|$ for the first variable $S_p(t)$, we have

$$\frac{1}{2}(e-\overline{e})^2(t_f) + \zeta_1\int_{t_0}^{t_f}(e-\overline{e})^2 d$$

$$\le \int_{t_0}^{t_f}\mu|e-\overline{e}|^2\,dt + \left[\int_{t_0}^{t_f}\left|q_1^*e - \overline{q}_1^*\overline{e}\right||e-\overline{e}|\,dt\right] + g^{\delta t}k\int_{t_0}^{t_f}|f-\overline{f}||e-\overline{e}|\,dt + \int_{t_0}^{t_f}\left|q_1^*e - \overline{q}_1^*\overline{e}\right||e-\overline{e}|\,dt$$

$$\le \psi_1\int_{t_0}^{t_f}|e-\overline{e}|^2 + |p-\overline{p}|^2 + |m-\overline{m}|^2 + |x-\overline{x}|^2]dt + \psi_2 g^{\delta t_f}\int_{t_0}^{t_f}\left[|e-\overline{e}|^2 + |p-\overline{p}|^2 + |m-\overline{m}|^2 + |x-\overline{x}|^2\right]dt$$

where, the constants $\varphi_{i=1,2}$ depends on the coefficients and on the bounds on the state and adjoint variables. Combining the sixteen estimates, we arrived at the following inequalities:

$$\frac{1}{2}(t_f)\left[(e-\overline{e})^2 + (f-\overline{f})^2 + \ldots\ldots\ldots + (n-\overline{n})^2\right] + \frac{1}{2}(t_0)\left[(p-\overline{p})^2 + \ldots\ldots\ldots + (v-\overline{v})^2\right]$$

$$+\zeta\int_{t_0}^{t_f}\left[(e-\bar{e})^2+(f-\bar{f})^2+.....+(n-\bar{n})^2+(p-\bar{p})^2+.....+(v-\bar{v})^2\right]dt$$

$$\leq\left(\tilde{\psi}_1+\tilde{\psi}_2 e^{3\zeta t_f}\right)\int_{t_0}^{t_f}\left[(e-\bar{e})^2+(f-\bar{f})^2+.....+(p-\bar{p})^2+.....+(v-\bar{v})^2\right]dt$$

for all $t_0=0$. Thus, we deduce from the above expression that

$$\left(\zeta-\tilde{\psi}_1+\tilde{\psi}_2 e^{3\zeta t_f}\right)\int_{t_0}^{t_f}\left[(e-\bar{e})^2+(f-\bar{f})^2+.....+(p-\bar{p})^2+.....+(v-\bar{v})^2\right]dt\leq 0,$$

where $\tilde{\psi}_1,\tilde{\psi}_2$ depends on the coefficients and bounds on $e, f, ..., x, v$. The last inequality can be simplified if we choose ζ such that $\zeta>\tilde{\psi}_1+\tilde{\psi}_2$ and $t_f<\frac{1}{3\zeta}\ln\left(\frac{\zeta-\tilde{\psi}_1}{\tilde{\psi}_2}\right)$, then $e=\bar{e}, f=\bar{f}, h=\bar{h}, ..., n=\bar{n}, ..., v=\bar{v}$. Therefore, for sufficiently small time interval t, the solution is unique.

Remark 3

The following observations are inferred:

i. Uniqueness of optimality system given by sufficiently small time is a two-point boundary value problem in nature.

ii. Optimal controls $q_{i=1,..,4}$ are characterized by the uniqueness of solution of optimality system.

iii. Optimal controls projects optimal treatment strategy for COVID-19 infection under designated dual-bilinear control functions.

5. Numerical simulations

Since it is imperative to analytically account for our derived optimality system, we resort to numerical simulations as the convenient approach for approximate evaluation of the dynamics of derived COVID-19 model. That is, to evaluate the viability of the present model in relation to it motivating model [8], we generate Tables 1 and 2 from our motivating model with the inclusion of parameters in line with our optimal control strategy. Thus, the numerical values for the present model are as in Tables 1 and 2 below:

Table 1. Description of state variables with values – model (4)

	Dependent variables	Initial values	Units
	Description		
S_p	Susceptible population to COVID-19 infection	0.5	
X_p	Exposed population	0.3	
A_u	Unaware asymptotic infectious population	0.1	
I_a	Aware infective population	0.15	***cells/ml*^{3}**
I_s	Isolated infectious population	0.0	
S_s	Super-spreaders infectious population	0.05	
H_i	Hospitalized infectious population	0.0	
R_p	COVID-19 recovered population	0.0	

Note: Table 1 is extracted and modified from models [1, 8]

Table 2. Description of constants and parameter values for model (4)

Parameter symbols	Parameters and constants Description	Initial values	Units
b_p	Source rate of susceptible population	$b_p \le 10.5$	ml^3d^{-1}
μ	Natural death rate for all sub-population	0.1	
k	Clearance rate of virus	0.25	
$\alpha_{i(i=1,..,5)}$	Death rates due infection at varying stages	0.2;0.3;0.1;0.4;0.5	day^{-1}
$\tau_{i=1,2}$	Rate at which I_a progresses to I_s and S_s	0.3, 0.5	
$C_{i(i=1,..,5)}$	Rates of contact of susceptible with various infectious stages	0.5;0.4;0.3;0.2;0.1	
$\eta_{i=1,2,3}$	Rates of recovery from H_i, I_s and S_s	0.5; 0.27;0.13	
$\beta_{i(1,..,5)}$	Probability of interactions of susceptible with varying Infectious classes	0.32;0.27;0.175; 0.125;0.05	$ml^3vir^{-1}d^{-1}$
$\varphi_{i=1,2}$	Proportions of A_u that progresses to H_i and S_s	0.3;0.18	
λ	Proportion of X_p becoming A_u	0.58	
θ	Proportion of A_u becoming I_a	0.32	
$\sigma_{i=1,2}$	Proliferations of recovered population to susceptible	0.14;0.6	
γ_s	Proportion of S_s progressing to I_s	0.22	ml^3d^{-1}
δ_h	Proportion of I_s progressing to H_i	0.14	
ρ_1	Proportion of I_a that progresses to I_s	0.34	
ρ_2	Proportion of I_a that progresses to H_i	0.48	
$(1-\rho_1-\rho_2)$	Proportion of I_a that progresses to S_s	0.08	
$q_{i=1,2}(t)$	Rates of use of face mask and social distancing	$q^*_{i=1,2}(t) \ge 0$	
$q_{i=3,4}(t)$	Treatment control functions (HCQ and AZT)	$q^*_{i=3,4}(t) \ge 0$	
$a_{i=1,..,4}$	Initial conditions for control functions	0.1,0.2,0.1,0.4	
$b_{i=1,..,4}$	Terminal conditions for control functions	0.4,0.9,0.4,0.7	
$Z_{i=1,..,4}$	Optimal weight factors	25000, 250, 25000, 250	

Note: Table 2 is clinically generated from certified data of [8, 18]

Moreso, we simulate our basic model for off-treatment scenario (i.e., $q_i^*(t)=0$) in comparison to the present derived optimality system under optimal control functions (i.e., $q_i^*(t)>0$) respectively. It is important to note that the entire simulations are performed using in-built Runge-Kutta of order of precision 4 in a Mathcad surface with the initial adjoint variables $\zeta_i > 0$.

5.1 Simulations of basic model and derived optimality system

We conductor numerical simulations for system (4) and eq. (17), which serves for zero optimal control functions and under application of optimal treatments. This is aim at providing suitable result for comparison for $q_i^*(t) \ge 0$. Thus, using Tables 1 and 2, we simulate as depicted by Figs 2(a1-h1) and 2(a2-h2) below:

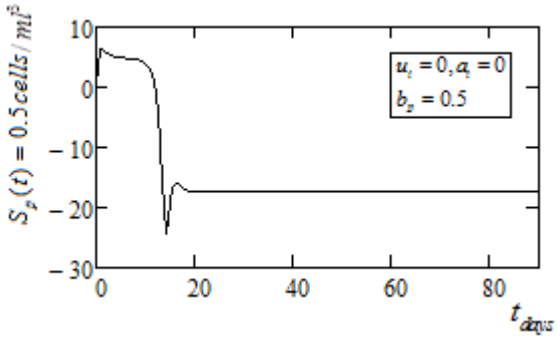

a1) Susceptible popn. under COVID-19 off-treatment scenario, $\mu = 0.1day^{-1}$

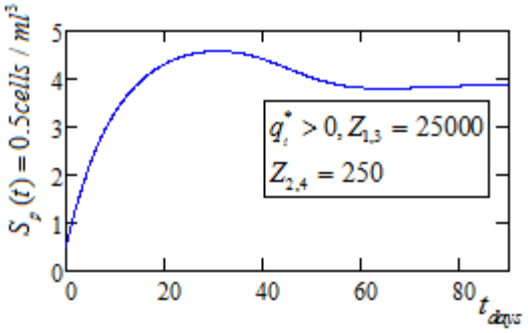

a2) Susceptible popn. under COVID-19 optimal treatment, $b_p = 0.5ml^3d^{-1}$

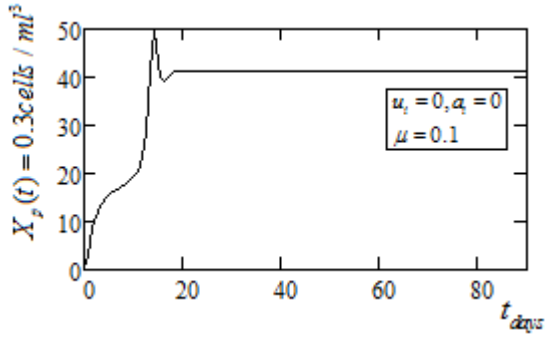

b1) Exposed popn. under COVID-19 off-treatment scenario, $\beta_i(\hat{N}) = 0.022$

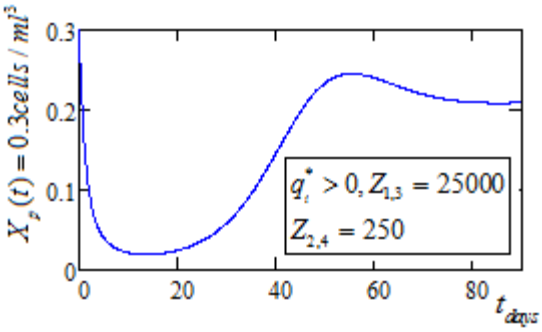

b2) Exposed COVID-19 popn. under optimal treatment, $\mu = 0.1day^{-1}$

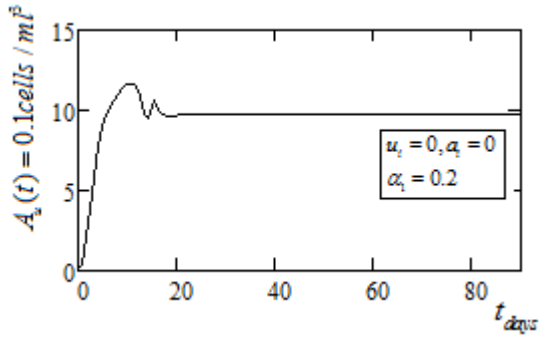

c1) Unaware asymptomatic infectious popn. under off-treatment, $\beta_i(\hat{N}) = 0.022$

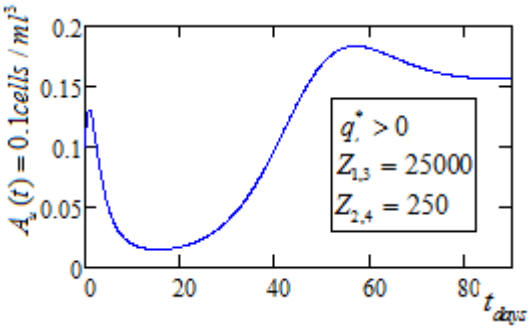

c2) Unaware asymptomatic infective popn. under optimal treatment, $\alpha_1 = 0.2d^{-1}$

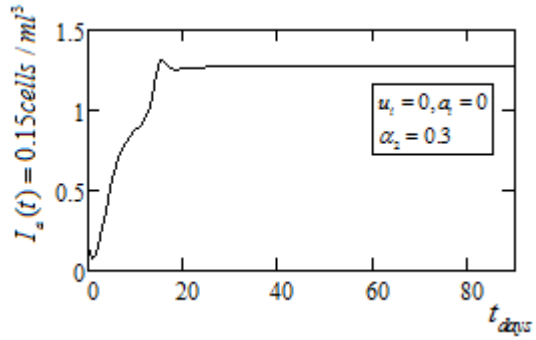

d1) Aware infective popn. under off-treatment scenario, $\beta_i(\hat{N}) = 0.022$

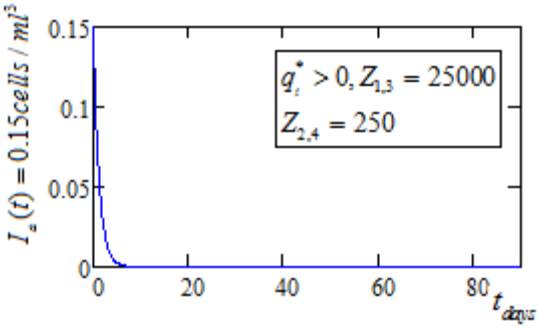

d2) Aware infective popn. under under optimal treatment, $\alpha_2 = 0.3d^{-1}$

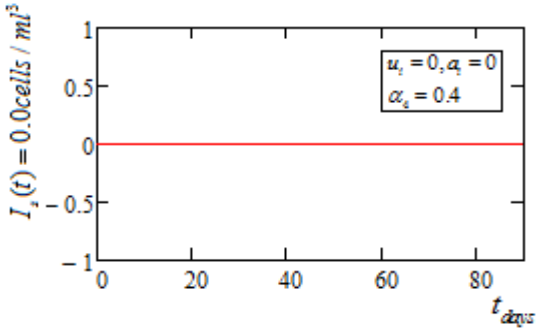

e1) Isolated infected popn. under off-treatment scenario, $\beta_i(\hat{N}) = 0.022$

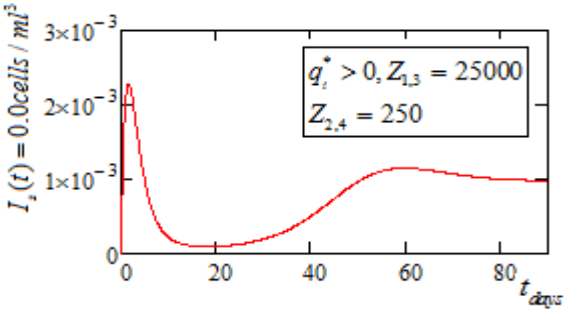

e2) Isolated infected popn. under optimal treatment, $\alpha_4 = 0.4d^{-1}$

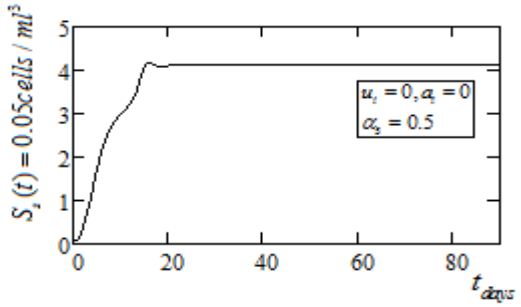

f1) Super spreaders under off-treatment scenario, $\beta_i(\hat{N}) = 0.022$

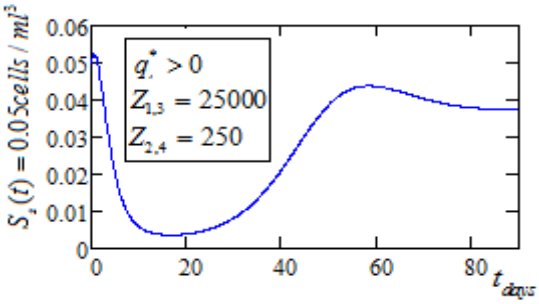

f2) Super spreaders under optimal treatment, $\alpha_5 = 0.5d^{-1}$

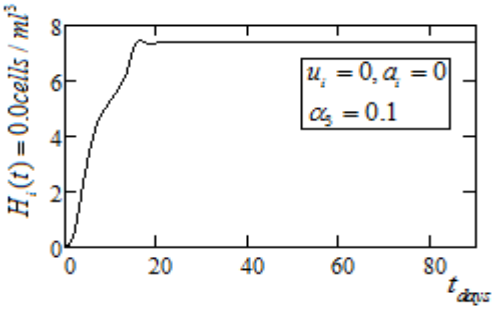

g1) Hospitalized popn. under off-treatment scenario, $\beta_i(\hat{N}) = 0.022$

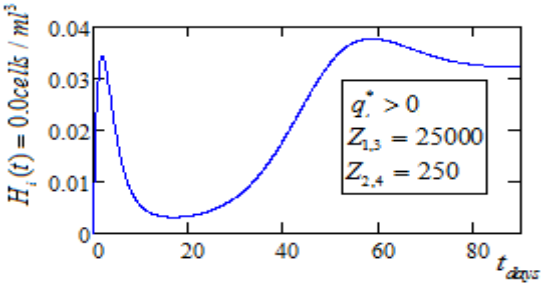

g2) Hospitalized popn. under optimal treatment, $\alpha_3 = 0.1d^{-1}$

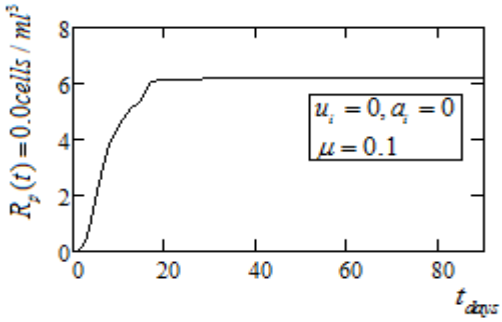

h1) Recovered popn. under off-treatment scenario, $\beta_i(\hat{N}) = 0.022$

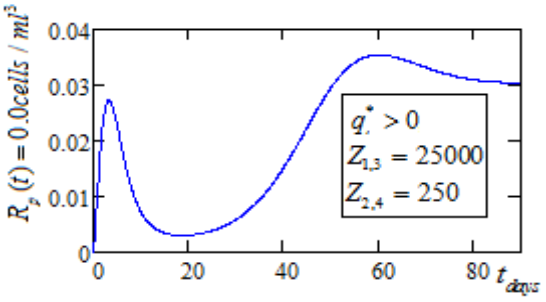

h2) Recovered popn. under optimal treatment, $\mu = 0.1d^{-1}$

Figure 2. (a1-h1) represent simulations of COVID-19 infection dynamics under off-treatment scenario with $u_{i=1,2} = 0, a_{i=1,2} = 0$ and $\beta_i(\hat{N}) = 0.022$; (a2-h2) represent simulations of COVID-19 infection dynamics under optimal treatments with, $q_{i=1,\ldots,4}^* > 0$

Comparatively, Fig. 2(a1) depicts the susceptible population at off-treatment scenario. Here, we observe complete contamination of the susceptible within the first 18 days i.e., $0.5 \le S_p(t) \le -24.447 cells/ml^3$ $18 \le t_f \le 90$ days. At optimal application of dual-bilinear control functions $q_i^*(t) > 0, i = 1,..,4$, we observe from Fig. 2(a2) rejuvenation of the susceptible population with incline value in the range of $0.5 \le S_p(t) \le 4.579 cells/ml^3$ at $t_f \le 38$ days and then attaining stability of $S_p(t) \le 3.9 cells/ml^3$ at $60 \le t_f \le 90$ days. From Fig. 2(b1), we simulate the dynamics of exposed population under off-treatment. We observe rapid exponential increase in the rate at which the susceptible become exposed with value range of $0.3 \le X_p(t) \le 59.785 cells/ml^3$ at $t_f \le 18$ days and then attaining endemic stability of $X_p(t) \le 41.024 cells/ml^3$ for all $18 \le t_f \le 90$ days. Corresponding compartment under optimal treatment (Fig. 2(b2)) yields accelerated concave-like decline with value at $0.019 \le X_p(t) \le 0.3 cells/ml^3$ for all $t_f \le 18$ days and then exhibits slight undulating surge of $X_p \le 0.21 cells/ml^3$ at $58 \le t_f \le 90$ days.

In Fig. 2(c1), where no treatment is administered, the unaware asymptomatic infectious population increases rapidly with value in the range of $0.1 \le A_u(t) \le 11.675 cells/ml^3$ for the first 10 days and then decline slightly to near stable value $A_u(t) \le 9.8 cells/ml^3$ for all $20 \le t_f \le 90$ days. With optimal treatment, Fig. 2(c2) illustrates the asymptomatic infectious class exhibiting concave-like decline to $0.1 \le A_u(t) \le 0.015 cells/ml^3$ at $t_f \le 18$ days. The dynamics of this compartment further exhibits undulating inclination with value range of $0.152 \le A_u(t) \le 0.183 cells/ml^3$ at $20 \le t_f \le 90$ days. Notably, screen aware infectives population under off-treatment as simulated in Fig. 2(d1) exhibit unsteady slow inclination with value of $0.15 \le I_a(t) \le 1.312 cells/ml^3$, which by far is lower when compared to unaware infectives of Fig. 2(c1). Corresponding compartment for aware infectives under optimal treatment as in Fig. 2(d2) exhibits early rapid decline to near zero, i.e., $0.15 \ge I_a(t) \ge 0.0 cells/ml^3$ for all $t_f \le 3$ days and sustain the zero decline through $3 \le t_f \le 90$ days.

Fig. 2(e1) depicts zero isolated infectious population following zero treatment/control measure i.e., $I_s = 0.0 cells/ml^3$ at $t_f \le 90$ days. Corresponding isolated infectious population under optimal control protocols as portrait by Fig. 2(e2) exhibit initial instantaneous inclination with value of $0.0 \le I_s \le 2.284 \times 10^{-3} cells/ml^3$ at $t_f \le 3$ days and is then accompanied by rapid undulating decline to near zero i.e., $2.284 \times 10^{-3} \ge I_s \ge 1 \times 10^{-3} cells/ml^3$. For off-treatment scenario with zero isolation facilities, commensurate rise in the rate of super spreaders is seen in Fig. 2(f1) with value range of $0.05 \le S_s(t) \le 4.17 cells/ml^3$ at $18 \le t_f \le 90$ days. Under optimal treatment as in Fig. 2(f2), we observed this similar compartment of super spreaders exhibit rapid undulating concave-like decline with value at $0.052 \ge S_s(t) \ge 3.616 \times 10^{-3}$ $cells/ml^3$ for all $t_f \le 20$ days, followed by slight undulating inclination to $S_s(t) \le 0.038 cells/ml^3$ at $20 \le t_f \le 90$ days.

The dynamics of hospitalized patients under off-treatment illustrated by Fig. 2(g1) shows rapid concentration rate of hospitalization of the infectives with value in the range of $0.0 \le H_i(t) \le 7.463 cells/ml^3$ for all $18 \le t_f \le 90$ days. Hospitalized compartment under optimal treatment protocols indicates initial slight increase with $0.0 \le H_i(t) \le 0.035$ $cells/ml^3$ in time interval $t_f \le 3$ days and then exhibit concave-like undulating decline to $0.038 \ge H_i(t) \ge 0.023 cells/ml^3$ days for all $60 \le t_f \le 90$ days. Finally, Fig 2(h1) represent somewhat incline rate of recovery population under off-treatment scenario. This account for possible recovery from exposed, super spreaders hospitalized compartments, which can be further attributed to natural immune response from varying infectious patients. Under optimal control functions with optimal conditions, corresponding recovery compartment exhibit similar curve to that of hospitalized curve with off-treatment but with lower recovery ratio i.e., $0.0 \le R_p(t) \le 0.028 cells/ml^3$ at $t_f \le 3$ days. It is further observed that recovery population decline to value range of $0.03 \le R_p(t) \le 0.035 cells/ml^3$ for all $20 \le t_f \le 90$ days, which indicated the efficacy of applied dual-bilinear control functions.

Notably, the results obtained agree with practical situation in the sense that, if infectives at varying stages are exposed to corresponding level of treatment protocols, then the population of super spreaders, isolations and hospitalization will definitely reduce. A situation that could lead to corresponding reduction in the rate of recovery. Moreso, upon recovery, individuals are recruited to the susceptible population. Thus, the further rejuvenation of the susceptible population under dual-bilinear control functions [see Fig. 2(a2)]. This massive outcome can be attributed to the model design methodological treatment protocols studied under classical optimal techniques (combination of Hessian matrix and Pontryagin's maximum principle). Obviously, the present results provided an enhance version of the results from our motivating model [8].

6. Discussion

This paper considered the COVID-19 model by [8] from which an extended version was formulated as an 8-Dimesional deterministic differential COVID-19 dynamic model primed with the investigation of the impact of optimal control technique for the optimal treatment protocols of novel COVID-19, following the application of dual-bilinear control functions. That is, in limiting the spread of Coronavirus, the model adopted two-set of bilinear controls: a bilinear non-pharmaceutical (face-masking and social-distancing) and a bilinear pharmacotherapies (hydroxylchloroquine—HCQ and azithromycin—AZT). Model formulation was based on compartmental state variables constituted by susceptible—exposed—unaware asymptomatic infectious—screen aware infectious—isolated infectious—super spreaders—hospitalized infectious—recovered. In line with system set goal, the system basic model was transformed to an optimal control problem. The main assumption of the study is defined by the control functions $q_i^*(t) > 0, i = 1,..,4$ as functions of time variation and having antiviral effect on the aerosol viral load production.

As an optimal control problem, the model adopted the classical Pontryagin's maximum principle in conjunction with the Hessian matrix method in the derivation and analysis of system optimality conditions. We considered the model for off-optimal control and as an optimal control problem following the application of dual-bilinear controls. Numerical validations for system theoretical predictions were simulated using in-built Runge-Kutta of order of precision 4 in a Mathcad surface. Clearly, numerical simulations were concurrently conducted for both off-optimal approach and for optimal dual-bilinear treatment to unveil the essence of applied optimal control technique. The results obtained indicated that under off-treatment (off- optimal approach), the system exhibited rapid extinction of the susceptible population within the first 18 days of exponential spread of COVID-19 as depicted by Fig. 2(a1).

Notably, corresponding susceptible compartment under optimal treatment indicated tremendous rejuvenation of the susceptible population with maximal value of $0.5 \le S_p(t) \le 4.579 cells/ml^3$ for all $t_f \le 38$ days. These largely significant results are manifested in outcomes of the exposed, asymptomatic infectious, aware infectious and super spreaders, which showed varying exponential inclination in the spread of the virus under off-treatment scenario see Fig. 2(b1-f1). On the other hand, Fig. 2(b2-f2) depicted the benefits of the application of optimal control technique in the present of optimal treatment following the accelerated concave-like reduction of the spread of the virus. Of note, the aware infectives was drastically reduced and sustained at zero after first 3 days of cogent application of dual-bilinear control mechanism.

Comparatively, zero infection flow is observed in the isolated compartment, which vindicated off-treatment scenario as against the concave-like diminishment of isolated population under optimal treatment protocols—see Fig. 2(e1 and e2). On hospitalized compartment under off-treatment, the rate of hospitalization was on the increase as projected by Fig. 2(g1). Here, the recovery outcome can be attributed to the interruption of infection flow by varying individual natural adaptive immune response. Fig. 2(g2) portrait accelerated concave-like decline of the rate of hospitalized patients, which agree with treatment protocols and does prove the effectiveness of control measures. Moreso, these current results are manifestation of the efficacy of applied methodological optimal controls.

Furthermore, the results surpass the outcome of same model by [8], where on-set treatment devoid of optimal control technique was applied. The high rate of hospitalization for our motivating model also vindicated the power of optimal control strategy as seen with low rate of hospitalization for the present model. The study have thus, ascertained the potential of optimal control as an important tool in the maximization of desired system state variables particularly for infectious diseases with conceptual medical vaccines.

7. Conclusion

In this paper, optimal control technique has been applied to investigate the impact of the tool for the maximization of COVID-19 predominant state variables following the methodological application of dual-bilinear optimal control functions. We defined the system control set including controlling the transmission of the viral load from unaware asymptomatic infectives to screen aware infectives, from aware infectives to super spreaders, isolated and hospitalized infectious populations. We investigated the mathematical characterization of the system optimal controls and then proved the existence of optimal controls for COVID-19. Furthermore, utilizing classical Pontryagin's maximum principle in conjunction with Hessian matrix, the study sought and determined the optimality system and investigated the uniqueness of the optimality system. Numerical validations of the system theoretical predictions were sequentially conducted in two folds: basic model under off-treatment scenario and the model optimality system under optimal treatment protocols. Numerical results obtained indicated that under off-treatment (off-optimal controls), the basic model exhibited rapid extinction of the susceptible population in the first 18 days. On the contrary, the application of optimal control technique under dual-bilinear control functions $q_{i=1,..,4}^*(t) > 0$, yields optimum impact with maximal recovery rate, tremendous rejuvenation of the susceptible population and near zero minimization of the spread of the deadly COVID-19 within minimal systemic cost for all

$t_f \leq 18$ days.

Of note, the results of the present study are by far an improvement when compared to the outcome from [8], where aware infectives under non-optimal control technique was not reduced to zero value. Thus, the use of optimal control techniques as a powerful tool has been unveiled by the enhanced result in the treatment and control of COVID-19 pandemic. Therefore, the application of optimal control techniques in relation to treatment of infectious diseases with particular attention to infections with no outright medical cure/vaccines is highly recommended.

Declarations: Funding and/or Conflicts of interests

The author otherwise known as the corresponding author declared a no conflict of interest and no funding received for this submitted manuscript. Moreso, the work described was an original research that has not been published previously and not under any consideration for publication elsewhere.

References

[1] Torres, DFM, Ndaïrou, F, Area, I, Nieto, JJ. Mathematical modeling of COVID-19 transmission dynamics with a case study of Wuhan. *Chaos, Solitons and Fractals*, http://ees.elsevier.com; 2020 [accessed 02, September, 2020].

[2] Gumel, AB. (2020). Using mathematics to understand and control the coronavirus pandemic, https://opinion.premiumtimesng.com/2020/05/04/using-mathematics tounderstand-and-control-the-coronavirus-pandemic-by-abba-b-gumel/; 2020 [accessed 16, August, 2020].

[3] Nita, HS, Ankush, HS, Ekta, NJ. (2020). Control strategies to curtail transmission of COCID-19. *Intl. J. Maths. and Mathcal. Sc.*, 2020; 1-12. http://downloads.hindawi.com/journals/ijmms/2020/2649514.pdf.

[4] World Health Organization. (2020). COVID-19 Weekly Epidemiological Update, https://www.who.int/publications/m/item/weekly-epidemiological-update---27-october-2020; 2020 [accessed 27, October, 2020].

[5] Nigeria Centre for Disease Control. (2020). Coronavirus disease (COVID-19) pandemic, https://ncdc.gov.ng/#; 2020 [accessed 27, October, 2020].

[6] Grigorieva, E, Khailov, E, Korobeinikov, A. (2020). Optimal quarantine strategies for COVID-19 control models. https://arxiv.org/pdf/ 2004.10614.pdf; 2020 [accessed 29, August, 2020].

[7] Leslie, M. (2020). T cells found in coronavirus patients 'bode well' for long-term immunity, http://science.sciencemag.org/ content/368/6493/809; 2020 [accessed 14, August, 2020].

[8] Bassey, E. B., Atsu, U. J. (2021). Global stability analysis of the role of multi-therapies and non-pharmaceutical treatment protocols for COVID-19 pandemic. *Chaos, Solitons and Fractals*, 143(2021), 110574. https://pubmed.ncbi.nlm.nih.gov/33519116/.

[9] Jahanshahi, H., Yousefpour, A., Bekires, S. (2020). Optimal policies for control of the novel coronavirus disease (COVID-19) outbreak. *Chaos, Solitons and Fractals*, 2020; 136: 1-6. https://www.ncbi.nlm.nih.gov/pmc/articles/PMC7229919/.

[10] Wu, JT, Leung, K, Leung, GM. (2020). Nowcasting and forecasting the potential domestic and international spread of the 2019.nCoV outbreak originating in Wuhan, China: a modeling study. *The Lacet* 2020; 395(10225):689-697. https://www.thelancet.com/action/showPdf?pii=S0140-6736%2820%2930260-9.

[11] Peng, L, Yang, W, Zhang, D, Zhuge, C, Hong, L. (2020). Epidemic analysis of COVID-19 in China by dynamical modeling, http://arxiv.org/abs/2002.06563; 2020 [accessed 14, August, 2020].

[12] Obsu, LL, Balcha, FS. (2020). Optimal control strategies for the transmission risk of COVID-19. *Journal of Biological Dynamics* 2020; 14(1): 590-607. https://www.tandfonline.com/doi/full/10.1080/17513758.2020.1788182.

[13] Moore, SE, Okyere, E. (2020). Controlling the transmission dynamics of COVID-19. *ArXiv*. 2020; 2004.00443, https://arxiv.org/pdf/2004.00443.pdf; 2020 [accessed 10 August, 2020].

[14] Sasmita, NR, Ikhwan, M, Suyanto, S, Chongsuvivatwong, V. (2020). Optimal control on a mathematical model to pattern the progression of coronavirus disease 2019 (COVID-19) in Indonesia. *Global Health Research and Policy* 2020; 5(38): 1-12. https://ghrp.biomedcentral.com/articles/10.1186/s41256-020-00163-2.

[15] Lee, D, Nasud, MA, Kim, BN, Oh, C. (2017). Optimal control analysis for the MEERS-CoV outbreak: South Korea perspectives. *J. Korea Soc. Indust. Appl. Math* 2017; 21(3): 143-154. http://koreascience.or.kr/article/JAKO201728441290805.pdf.

[16] Imai, N, Cori, A, Dorigatti, I, et al. (2020). MRC Centre for Global Infectious Disease Analysis: Wuhan coronavirus reports 1-3, https://www.imperial.ac.uk/media/imperial-college/medicine/sph/ide/gida-fellowships/Imperial-College-COVID19-transmissibility-25-01-2020.pdf; 2020 [accessed 21 November, 2020].

[17] Wahid, BKA, Moustapha, D, Rabi, HG, Bisso, S. (2020). Contribution to the Mathematical Modeling of COVID-19 in Niger. *Applied Mathematics* 2020; 11: 427-435. https://doi.org/10.4236/am.2020.116030.

[18] AL-Husseiny, HF, Mohsen, AA, Zhou, X. (2020). A dynamical behavior of COVID-19 virus model with carrier effect to Outbreak Epidemic. *Research Square//Preprint*, https://www.researchsquare.com/article/rs-24219/v1; 2020 [accessed 12, August, 2020].

[19] Danane, J, Allali, K. (2018). Mathematical Analysis and Treatment for a Delayed Hepatitis B Viral Infection Model with the Adaptive Immune Response and DNA-Containing Capsids. *High-Throughput* 2018; **7**(35): 1-16. https://www.ncbi.nlm.nih.gov/pmc/articles/PMC6306857/.

[20] Fister, KR, Lenhart, S, McNally, JS. (1998). Optimizing chemotherapy in an HIV Model. *Electr. J. Diff. Eq.* 1998; 32: 1-12. http://emis.matem.unam.mx/journals/EJDE/1998/32/fister.pdf

[21] Hattaf, K, Yousfi, N. (2012). Optimal control of a delayed HIV infection model with immune response using an efficient numerical method. *Biomathematics* 2012; 1-7. https://www.hindawi.com/journals/isrn/2012/215124/.

[22] Joshi, HR. (2002). Optimal Control of an HIV Immunology Model. *Optimal Control Applications and Methods* 2002; 23:199-213. http://www.math.utk.edu/~lenhart/docs/hiv.pdf.

[23] Kahuru, J, Luboobi, L, Nkansah-Gyekye, Y. (2017). Optimal control techniques on a mathematical model for the dynamics of tungiasis in a community. *Intl. J. Maths and Mathcal. Sc.* 2017; 1-9. https://www.hindawi.com/journals/ijmms/2017/4804897/.

[24] Bassey, EB. (2021). Optimal multi-therapeutic protocols for the control of cholera mortality rate. 39th Annual Conference of the Nigeria Mathematical Society (NMS-RUN 2020), C40:(46). Retrieved date: [12, April, 2021], online available at https://www.app.nigerianmathematicalsociety.org/conference.

[25] Fleming, W, Rishel, R. (1975). *Deterministic and Stochastic Optimal Control*. Springer Verlag: New York; 1975. http://dx.doi.org/10.1007/978-1-4612- 6380-7.

[26] Culshaw, R, Ruan, S, Spiteri, RJ. (2004). Optimal HIV Treatment by Maximizing Immune Response. *Journal of Mathematical Biology* 2004; 48(5): 545-562. https://miami.pure.elsevier.com/en/publications/optimal-hiv-treatment-by-maximising-immune-response.

[27] Bassey, BE. (2020). Optimal control dynamics: Multi-therapies with dual immune response for treatment of dual delayed HIV-HBV Infections. *I.J. Mathematical Sciences and Computing* 2020*c*; 6(2):18-60. http://www.mecs-press.org/ijmsc/ijmsc-v6-n2/IJMSC-V6-N2-2.pdf

[28] Pontryagin, LS, Boltyanskii, VG, Gamkrelize, RV, Mishchenko, EF. (1967). *The Mathematical Theory of Optimal Processes.* Wiley: New York; 1967. https://onlinelibrary.wiley.com/doi/abs/10.1002/zamm.19630431023.